

# Characterization of Picosecond Pulse Crosstalk Between Coupled Microstrip Lines with Arbitrary Conductor Width

Yongxi Qian, *Student Member, IEEE*, and Eikichi Yamashita, *Fellow, IEEE*

**Abstract**—The propagation and crosstalk properties of picosecond electrical pulses along coupled microstrip lines with arbitrary strip widths are investigated. The current distributions and propagation constants of the dominant  $c$ - and  $\pi$ -modes in these asymmetric coupled striplines are calculated by using the spectral domain approach; and the full-wave analysis results obtained are incorporated into an FFT algorithm to simulate pulse distortion and crosstalk in the coupled transmission lines. Several samples of asymmetric coupled microstrip lines are fabricated and their characteristics are measured. The results of experiments are found to be in good agreement with those of computer simulations. This paper provides, for the first time, rigorous results of picosecond pulse distortion and crosstalk in asymmetric coupled transmission lines.

## I. INTRODUCTION

As smaller interline spacings and higher integration densities are required for further development of MMIC's and high-speed digital circuits, the effect of signal coupling between adjacent transmission lines becomes a problem of critical importance. For the transmission of pulses with ultrashort durations, the existence of closely located strip conductors will introduce coupling distortion to the signal pulse in addition to the intrinsic frequency dispersion and propagation attenuations, and will cause unexpected crosstalk to the neighboring lines.

Early studies of pulse coupling and crosstalk were almost exclusively based on the TEM approximation [1], [2]. As shorter pulses with picosecond durations are employed to realize increased signal information, full-wave analyses are required for the accurate characterization of pulse behaviors in these transmission lines. For this purpose, the spectral domain approach has often been used to obtain the frequency-dependent phase velocities of the propagation modes [3]–[5]. Time-domain investigation of pulse distortion including both frequency and coupling dispersion effects was first reported by Gilb and Balanis [6], where an even- and odd-mode approach was applied for simulations of pulse propagation and crosstalk in a pair of symmetric coupled microstrip lines. Carin and Webb [7] have studied pulse isolation effects by introducing grounded isolation lines. Pulse distortion and coupling in lossy coupled lines [8] and dispersion characteristics of square

pulses with finite rise time in coupled microstrip lines [9] have also been reported recently.

Since the coupled transmission lines investigated in the above-mentioned literature were almost exclusively of symmetric geometries, the even- and odd-mode approach can be simply applied. For the general case of coupled lines with arbitrary strip widths, however, the problem becomes more complicated since the current distributions as well as the amplitudes of current densities on the conductors are no longer the same. It is required that the current distributions on each strip conductor be treated independently, and the coefficients of the current densities be computed after the propagation constants of the coupling modes have been determined [10]. To the authors' knowledge, there have been no detailed reports characterizing pulse propagation in these generalized coupled transmission lines.

In this paper we concentrate on the studies of pulse propagation and crosstalk in a pair of asymmetric coupled microstrip lines. The current distributions (eigenfunctions) as well as propagation constants (eigenvalues) of the dominant  $c$ - and  $\pi$ -modes are first calculated by using the spectral domain approach. The results obtained with the full-wave analysis are incorporated into an FFT algorithm to study pulse distortion on the signal line and crosstalk to the adjacent line. Computer simulation results of pulse waveform evolution along coupled microstrip lines of various interline spacings are presented. We have also fabricated several patterns of asymmetric coupled microstrip lines for the experimental evaluation of pulse distortion and crosstalk. A fairly good agreement has been found between the measured pulse waveforms and those of computer simulations.

## II. FULL-WAVE ANALYSIS

Fig. 1 shows the cross-sectional view and geometries of the asymmetric microstrip lines under investigation. The two strip conductors are assumed to be negligibly thin and perfectly conducting, and the dielectric substrate is lossless and isotropic. This transmission line structure can be readily analyzed by using the spectral domain approach. Details of the numerical method are not repeated here since they have been well documented in the open literature [11]. We concentrate our study on the current distributions on the strip conductors. Since  $w_1$  and  $w_2$  are different, there is no longer any symmetry in the current distributions on the two lines, and the current densities

Manuscript received July 27, 1992; revised October 20, 1992.  
The authors are with the Department of Electronic Engineering, University of Electro-communications, Chofu-shi, Tokyo, 182 Japan.  
IEEE Log Number 9208364.

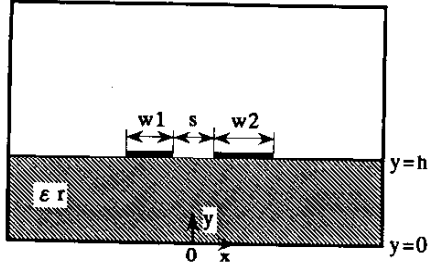


Fig. 1. Cross-sectional view and geometries of the asymmetric coupled microstrip lines for analysis.

must be expanded with independent basis functions. Referring to Fig. 1, we can assume the longitudinal and transversal components of the current density in the air-dielectric interface plane to be

$$J_z(x) = \begin{cases} \sum_{m=1}^{N_1} c_{1m} J_{1zm}(x) & -(b_1 + w_1/2) < x < -(b_1 - w_1/2) \\ \sum_{m=1}^{N_2} c_{2m} J_{2zm}(x) & b_2 - w_2/2 < x < b_2 + w_2/2 \end{cases} \quad (1a)$$

$$J_x(x) = \begin{cases} \sum_{m=1}^{M_1} d_{1m} J_{1xm}(x) & -(b_1 + w_1/2) < x < -(b_1 - w_1/2) \\ \sum_{m=1}^{M_2} d_{2m} J_{2xm}(x) & b_2 - w_2/2 < x < b_2 + w_2/2 \end{cases} \quad (1b)$$

where  $b_1 = (s + w_1)/2$ ,  $b_2 = (s + w_2)/2$ , and  $c_{1m}$ ,  $c_{2m}$ ,  $d_{1m}$ , and  $d_{2m}$  are unknown coefficients. The basis functions are chosen as follows:

$$J_{1zn}(x) = \frac{T_n[2(x + b_1)/w_1]}{\sqrt{1 - [2(x + b_1)/w_1]^2}} \quad (2a)$$

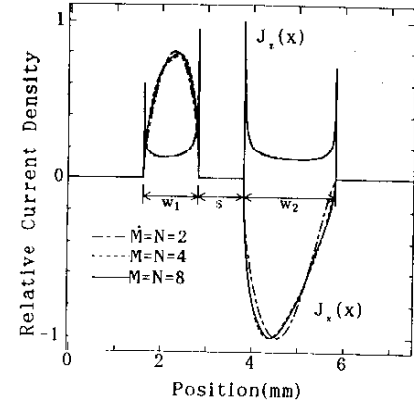
$$J_{2zn}(x) = \frac{T_n[2(x - b_2)/w_2]}{\sqrt{1 - [2(x - b_2)/w_2]^2}} \quad (2b)$$

$$J_{1xn}(x) = jU_n[2(x + b_1)/w_1] \sqrt{1 - [2(x + b_1)/w_1]^2} \quad (2c)$$

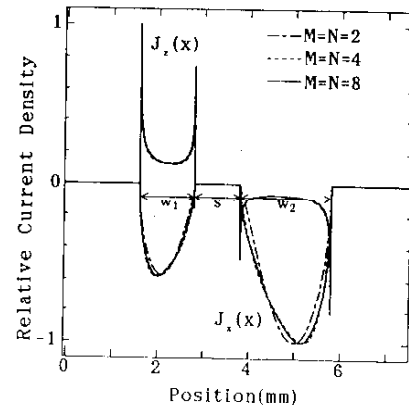
$$J_{2xn}(x) = jU_n[2(x - b_2)/w_2] \sqrt{1 - [2(x - b_2)/w_2]^2} \quad (2d)$$

where  $T_n(x)$  and  $U_n(x)$  are Chebyshev polynomials of the first and second kind, respectively. The Fourier transforms of these basis functions are readily expressed in closed forms [10], which are employed to form a set of homogeneous equations for obtaining the propagation constant (eigenvalues) and current densities (eigenfunctions) in the coupled lines structure.

For a pair of asymmetric coupled microstrip lines, the dominant propagation modes are the  $c$ - and  $\pi$ -modes, whose longitudinal current densities are in-phase and out-of-phase, respectively, just as with the even and odd modes for the case of symmetric structures. Fig. 2 plots the normalized longitudinal and transverse current distributions of the  $c$ - and  $\pi$ -modes for several values of the number of basis functions ( $M = N = 2, 4, 8$ ) at the frequency of 1 GHz. The dimensions



(a)



(b)

Fig. 2. Convergence of strip current distributions with respect to the number of basis functions: (a)  $c$ -mode and (b)  $\pi$ -mode. (Other parameters:  $w_1 = 1.2$  mm,  $w_2 = 2.0$  mm,  $s = 1.0$  mm,  $h = 1.3$  mm,  $\epsilon_r = 10.5$ , and  $f = 1$  GHz.)

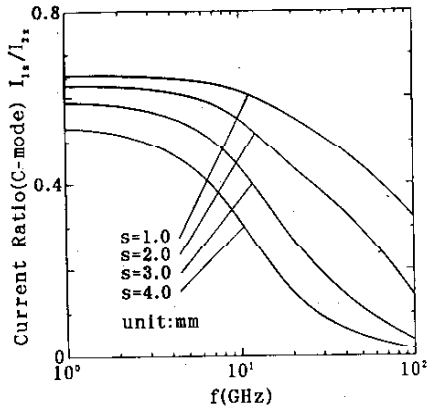
of the coupled lines structure are:  $w_1 = 1.2$  mm,  $w_2 = 2.0$  mm,  $s = 1.0$  mm,  $h = 1.3$  mm, and  $\epsilon_r = 10.5$ . It is seen that a very good convergence of the longitudinal current distribution is obtained when  $M = N = 2$ , while the convergence of the transverse current requires  $M = N = 4$  for the present structure. A greater number of basis functions will be required with increased frequency, as has also been discussed by Kobayashi *et al.* [12].

After the current distributions are obtained, they are integrated over the strip width to give the total currents on the conductors. The longitudinal currents on the two microstrip lines,  $I_{1z}$  and  $I_{2z}$ , can be calculated as follows:

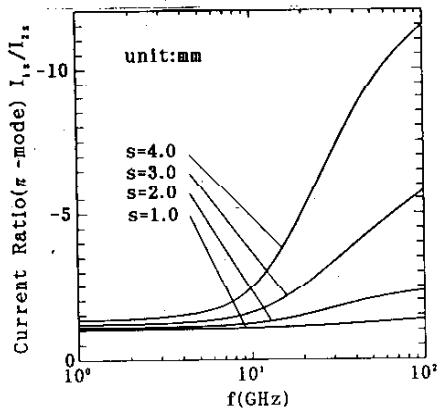
$$I_{1z} = \sum_{m=0}^{N_1} c_{1m} \int_{-(b_1 + w_1/2)}^{-(b_1 - w_1/2)} J_{1zm}(x) dx \quad (3a)$$

$$I_{2z} = \sum_{m=0}^{N_2} c_{2m} \int_{b_2 - w_2/2}^{b_2 + w_2/2} J_{2zm}(x) dx. \quad (3b)$$

For the case of symmetric coupled lines, we have  $I_{1z} = I_{2z}$  for the even mode and  $I_{1z} = -I_{2z}$  for the odd mode at all frequencies. When the two coupled lines are not identical, the current distributions are no longer symmetric, and the current ratio,  $I_{1z}/I_{2z}$ , is not constant for different frequencies. Fig. 3 shows the frequency-dependent current ratios for the



(a)



(b)

Fig. 3. Frequency-dependent propagation constant for the *c*- and  $\pi$ -mode in asymmetric coupled microstrip line.

*c*- and  $\pi$ -mode, respectively. Note that the current ratios in Fig. 3(b) are of negative values, which reveals the out-of-phase characteristics of the longitudinal current densities for the  $\pi$ -mode. For the case of traveling wave propagation, these current ratios are identical to the ratios of voltage amplitude, which are important parameters for time-domain simulations of pulse propagation and crosstalk in asymmetric coupled microstrip lines.

Fig. 4 shows the numerical results of the normalized propagation constant,  $\beta/\beta_0$ , of the *c*- and  $\pi$ -modes for several values of line spacings, *s*. The frequency dependence of the propagation constant can be approximated by the following empirical formula through a least-square curve-fitting procedure [13]:

$$\frac{\beta}{\beta_0} = \frac{\sqrt{\epsilon_r} - \beta_{TEM}/\beta_0}{1 + aF^{-b}} + \frac{\beta_{TEM}}{\beta_0} \quad (4)$$

where  $F = (f/c)4h\sqrt{\epsilon_r - 1}$  is the normalized frequency,  $\beta_{TEM}$  is the propagation constant assuming the quasi-TEM approximation, and *a* and *b* are constants which depend on the dimensions of the transmission line. For the case of *s* = 1.0 mm, we obtain *a* = 0.466, *b* = 1.562 for the *c*-mode, and *a* = 1.319, *b* = 1.978 for the  $\pi$ -mode, and the above formula is accurate to within 1% in the frequency range 1–100 GHz.

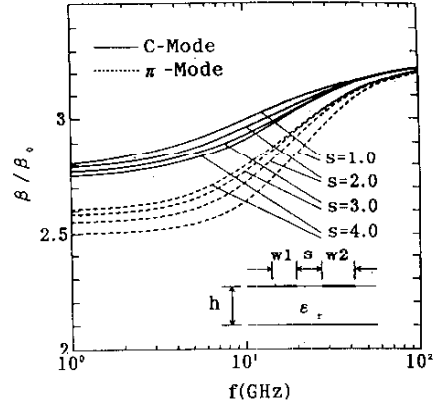


Fig. 4. Frequency-dependent ratio of longitudinal current densities in asymmetric coupled microstrip lines: (a) *c*-mode and (b)  $\pi$ -mode.

### III. COMPUTER SIMULATIONS OF PULSE PROPAGATION

For a pair of symmetric coupled transmission lines, there is a simple way of analyzing the pulse response by splitting the input signal into even and odd modes. In the even mode, two in-phase signals are launched into both of the microstrip lines, while in the odd mode, the same two signals are fed but are 180 degrees out of phase with each other [9]. In the case of asymmetric coupled microstrip lines, however, the amplitudes of the current densities on the conductors are not the same. In general, to completely characterize an *N*-conductor system, it is necessary to determine *N* different propagation constants and an *N* by *N* matrix,  $[A(\omega)]$ , that specifies the relative magnitudes of the current densities on each of the *N* conductors for each of the *N* modes at the angular frequency  $\omega$  [10]. If we define the ratios of current densities shown in Fig. 3(a) and (b) to be  $a_{2c}(\omega)$  and  $a_{2\pi}(\omega)$ , respectively, we have

$$[A(\omega)] = \begin{bmatrix} 1 & 1 \\ a_{2c}(\omega) & a_{2\pi}(\omega) \end{bmatrix} \quad (5)$$

which is also true in describing the ratios of voltage amplitudes on the conductors. On the other hand, to characterize pulse propagation and crosstalk along the coupled lines, it is necessary to find a linear combination of the *c*- and  $\pi$ -mode which gives a unit amplitude signal on one line and no signal on the other. This linear combination can be expressed by the following matrix:

$$[C(\omega)] = \begin{bmatrix} c_{c1} & c_{c2} \\ c_{\pi1} & c_{\pi2} \end{bmatrix} \quad (6)$$

which, according to [10], is simply the inverse of the current coefficient matrix,  $[A(\omega)]$ . Since  $a_{2c}$  and  $a_{2\pi}$  have been numerically calculated over the frequency range of interest, the constants of linear combination are readily obtained as follows:

$$\begin{bmatrix} c_{c1} & c_{c2} \\ c_{\pi1} & c_{\pi2} \end{bmatrix} = \begin{bmatrix} 1 & 1 \\ a_{2c} & a_{2\pi} \end{bmatrix}^{-1} \quad (7)$$

The computer simulation of pulse propagation and crosstalk is carried out by using an algorithm similar to that described

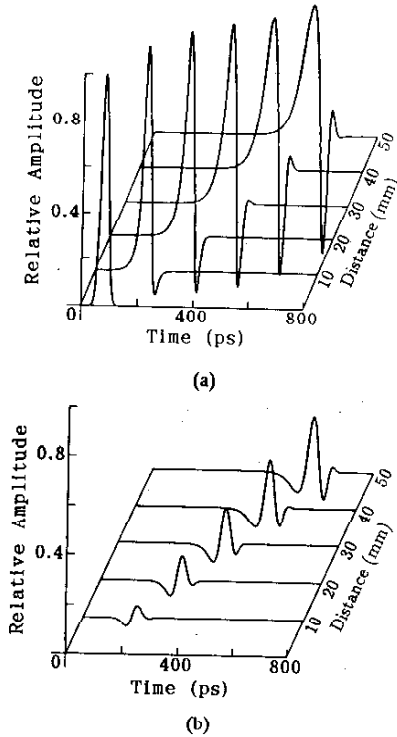


Fig. 5. Computer simulation results of the propagation of a 30 ps (FWHM) Gaussian pulse along asymmetric coupled microstrips with  $s = 4.0$  mm: (a) signal line and (b) neighboring line.

in [14]. We used the following Gaussian pulse as the input signal to line 1:

$$v(0, t) = V_0 e^{-4 \ln 2 (t/\tau)^2} \quad (8)$$

where  $\tau$  represents the FWHM (Full Width at Half Maximum) of the pulse. The input signal is Fourier-transformed into its frequency spectrum,  $\tilde{V}(\omega)$ . Multiplying this by the appropriate coefficients of the linear combination and current amplitude as well as the propagation factor,  $\gamma(\omega)$ , and taking an inverse Fourier transform, we obtain the pulse response on the two lines after a propagation distance of  $L$  as follows:

$$v_1(L, t) = \mathcal{F}^{-1} \{ c_{c1}(\omega) \tilde{V}(\omega) e^{-\gamma_c(\omega)L} + c_{\pi 1}(\omega) \tilde{V}(\omega) e^{-\gamma_\pi(\omega)L} \} \quad (9a)$$

$$v_2(L, t) = \mathcal{F}^{-1} \{ a_{2c}(\omega) c_{c2}(\omega) \tilde{V}(\omega) e^{-\gamma_c(\omega)L} + a_{2\pi}(\omega) c_{\pi 2}(\omega) \tilde{V}(\omega) e^{-\gamma_\pi(\omega)L} \} \quad (9b)$$

where  $\mathcal{F}^{-1}$  denotes the inverse Fourier transform, and  $\gamma_i(\omega)$  ( $i = c, \pi$ ) is the propagation constant for the  $c$ - and  $\pi$ -mode, respectively. A complete description of  $\gamma_i(\omega)$  should include both the attenuation constant,  $\alpha_i(\omega)$ , as well as the phase constant,  $\beta_i(\omega)$ . Since in this paper we are considering pulses of a few tens of picoseconds, whose frequency components are also within a few tens of gigahertz, signal attenuation due to conductor and dielectric losses as well as radiation losses is usually small and can be neglected without much influence on the simulation results of pulse propagation [15]. For simplicity, only the imaginary part of the propagation constant,  $\beta_i(\omega)$ , has been considered in the simulation program.

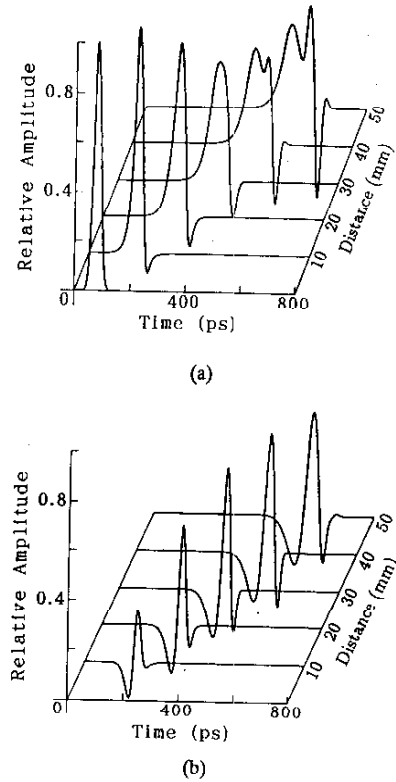


Fig. 6. Computer simulation results of the propagation of a 30 ps (FWHM) Gaussian pulse along asymmetric coupled microstrips with  $s = 1.0$  mm: (a) signal line and (b) neighboring line.

Figs. 5 and 6 show some of the computer simulation results of the distortion as well as crosstalk of a Gaussian pulse along two pairs of asymmetric coupled microstrip lines with line spacings of 4 and 1 mm, respectively. The input signal, which is a 30 ps (FWHM) Gaussian pulse with a rise time (10–90%) of 22 ps, is sent down line 1. The distorted pulse on the signal line and crosstalk pulse to the neighboring line are plotted at several different locations along the coupled lines. When the two lines are separated by a relatively large distance, the coupling effect is weak. There is only a small crosstalk to the adjacent line, and pulse distortion along the signal line is similar to that in single microstrip lines. In Fig. 5, the 30 ps (FWHM) input Gaussian pulse is broadened to 65 ps (FWHM) and with a rising time of 83 ps after a propagation distance of 50 mm. The amplitude of the signal pulse is 56% of that of the original signal, and the crosstalk pulse has a peak amplitude of 23% of that of the input pulse.

Fig. 6 shows the pulse distortion and crosstalk along a pair of more tightly coupled lines with  $s = 1$  mm. Since the difference between the propagation constants of the  $c$ - and  $\pi$ -mode becomes larger with decreased interline spacings, as shown in Fig. 4, the signal pulse on line 1 experiences more broadening in pulsewidth. As can be seen in Fig. 6(a), the signal pulse is seriously distorted. After a propagation distance of 40 mm, the main peak is separated into two peaks because of the different traveling speeds of the  $c$ - and  $\pi$ -modes. The pulse width at  $L = 50$  mm is 117 ps, which is nearly 4 times

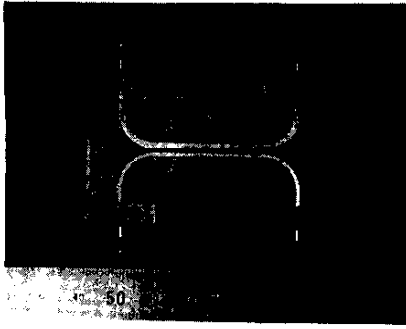


Fig. 7. Photograph of the asymmetric coupled microstrip lines fabricated for experiment measurements.

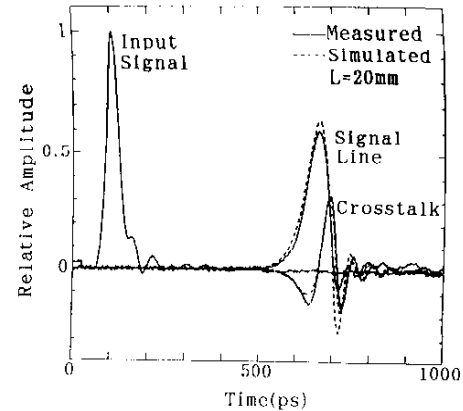
that of the input pulse (30 ps), and about 2 times broader than that of the signal pulse in Fig. 5(a). Meanwhile, the pulse crosstalk, as shown in Fig. 6(b), is also much more significant than the case of  $s = 4$  mm. The amplitude of the pulse on line 2 at  $L = 30$  mm is 49% of the amplitude of the original signal. Further propagation along the coupled lines makes no significant difference in the amplitude of the crosstalk pulse, but shows a gradual broadening in the pulsewidth.

#### IV. EXPERIMENTAL RESULTS

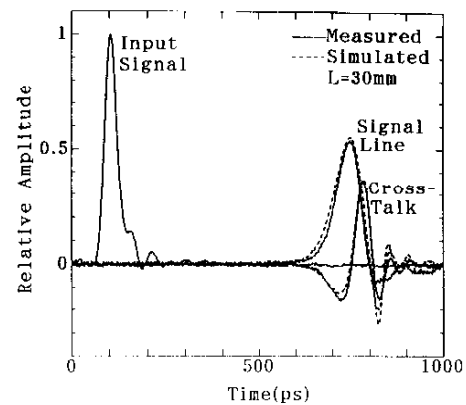
To confirm the validity of the theoretical predictions of pulse distortion and crosstalk effect, we fabricated several samples of asymmetric coupled microstrip lines for experimental measurements. Fig. 7 is the top-view photograph of one of the patterns fabricated. The two coupled lines, which are 1.2 and 2.0 mm wide, respectively, and 1 mm separated from each other, have a variable coupling length of  $L$ . The substrate is the DI-CLAD 810 produced by Arlon, which is 1.3 mm thick and has a dielectric constant of 10.5. To connect the microstrips to SMA connectors, 90 degree curved line sections are used to decouple the two microstrips at both ends. The 2.0-mm-wide line is linearly tapered at each end to offer a good match with the 50  $\Omega$  coaxial connectors.

In the experiment, the 1.2-mm-wide and 2.0-mm-wide lines are used as the signal line and neighboring coupled line, respectively. The experiment system is similar to that described in [16]. A Gaussian-like pulse of approximately 35 ps (FWHM) is launched into one port of the signal line, and the two ports on the other end are connected to the sampling heads of a digital oscilloscope (Tektronix 11802). The sampling oscilloscope is controlled via GPIB by a personal computer (NEC PC-9801) for data transference and processing. The sampling head of the oscilloscope (SD-30) has a frequency bandwidth of 40 GHz, which corresponds to a time resolution of 8.8 ps.

Fig. 8 shows some experimental as well as simulation results of pulse distortion and crosstalk along two pairs of fabricated coupled lines with  $L = 20$  and 30 mm, respectively. The same input pulse as for experiment was used for computer simulations in order to offer a rigorous comparison between theory and measurement. The 90 degree curved line sections were approximated by microstrip lines with equivalent lengths.



(a)



(b)

Fig. 8. Experimental (solid lines) and simulation (dotted lines) results of pulse propagation along the fabricated coupled microstrip lines: (a)  $L = 20$  mm and (b)  $L = 30$  mm.

In Fig. 8(a) and (b), the time delay of the measured pulses has been shifted slightly to compensate for the time offset caused at the SMA connecting parts. The reason for doing this is that all the measured pulses need the same time shift to lie atop those of computer simulations, while the relative delay time between two places along the coupled lines is the same for both experiment and simulation. As can be seen in Fig. 8, the input signal pulse experiences serious distortion and causes a substantial amount of crosstalk to the neighboring line as it propagates along the coupled microstrip lines. For the coupler pattern for  $L = 30$  mm, the output pulse on the signal line has broadened from 35 (FWHM) to 82 ps, the 10–90% rise time has expanded from 25 to 90 ps, and the voltage amplitude has dropped to 55% of that of the original pulse. Meanwhile, the crosstalk pulse on the neighboring line has reached an amplitude of about 37% of that of the input signal, which indicates a significant amount of crosstalk. While there exist some slight discrepancies between the computer simulated pulses and those of experimental measurements, which may have been caused by the approximate treatment of the curved and tapered line sections, the comparison as shown in Fig. 8(a) and (b) reveals a fairly good agreement in both waveforms and peak amplitudes, confirming the validity of the simulation procedures as described in the previous section.

## V. CONCLUSION

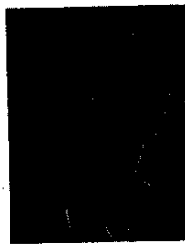
In this paper we have investigated the pulse propagation and crosstalk characteristics in a pair of coupled microstrips with arbitrary widths. By calculating the current distributions and propagation constants of the dominant  $c$ - and  $\pi$ -mode in these asymmetric coupled striplines using the spectral domain approach, and combining the full-wave analysis results with an FFT algorithm, we have been able to investigate pulse distortion and crosstalk in the coupled transmission lines through computer simulations. We have also fabricated several samples of asymmetric coupled microstrip lines to characterize pulse performance in these transmission line structures experimentally. For the first time, we offer a rigorous, quantitative comparison between theoretical and experimental results of picosecond pulse distortion and crosstalk in such kind of asymmetric coupled lines. Our experimental results are found to be in good agreement with those of computer simulations. The contents of the present paper can be readily extended to studies of more general, multiconductor interconnects in MMIC's or high-speed digital circuits.

## ACKNOWLEDGMENT

The authors wish to thank Prof. K. Atsuki for reviewing the manuscript, and Dr. N. Kishi, L. Zhu, and Z. Ma for their helpful discussions.

## REFERENCES

- [1] A. R. Djordjevic, T. K. Sarkar, and R. F. Harrington, "Analysis of lossy transmission lines with arbitrary nonlinear terminal networks," *IEEE Trans. Microwave Theory Tech.*, vol. MTT-34, pp. 660-666, June 1986.
- [2] V. K. Tripathi and J. B. Retting, "A SPICE model for multiple coupled microstrips and other transmission lines," *IEEE Trans. Microwave Theory Tech.*, vol. MTT-33, pp. 1513-1518, Dec. 1985.
- [3] R. H. Jansen, "Fast accurate hybrid mode computation of nonsymmetrical coupled microstrip characteristics," in *Proc. 7th Euro. Microwave Conf.*, Denmark, 1977, pp. 135-139.
- [4] Y. Fukuoka, Q. Zhang, D. P. Neikirk, and T. Itoh, "Analysis of multilayer interconnection lines for a high-speed digital integrated circuit," *IEEE Trans. Microwave Theory Tech.*, vol. MTT-33, pp. 527-532, June 1985.
- [5] E. G. Farr, C. H. Chan, and R. Mittra, "A frequency-dependent coupled-mode analysis of multiconductor microstrip lines with application to VLSI interconnection problems," *IEEE Trans. Microwave Theory Tech.*, vol. MTT-34, pp. 307-310, Feb. 1986.
- [6] J. P. Gilb and C. A. Balanis, "Pulse distortion on multilayer coupled microstrip lines," *IEEE Trans. Microwave Theory Tech.*, vol. MTT-37, pp. 1620-1627, Dec. 1989.
- [7] L. Carin and K. J. Webb, "Isolation effects in single- and dual-plane VLSI interconnects," *IEEE Trans. Microwave Theory Tech.*, vol. MTT-38, pp. 396-404, Apr. 1990.
- [8] J. P. K. Gilb and C. A. Balanis, "Transient analysis of distortion and coupling in lossy coupled microstrips," *IEEE Trans. Microwave Theory Tech.*, vol. MTT-38, pp. 1894-1899, Dec. 1990.
- [9] P. Pramanick and R. R. Mansour, "Dispersion characteristics of square pulse with finite rise time in single, tapered, and coupled microstrip lines," *IEEE Trans. Microwave Theory Tech.*, vol. MTT-39, pp. 2117-2122, Dec. 1991.
- [10] J. P. K. Gilb and C. A. Balanis, "Asymmetric, multi-conductor low-coupling structures for high-speed, high-density digital interconnect," *IEEE Trans. Microwave Theory Tech.*, vol. MTT-39, pp. 2100-2106, Dec. 1991.
- [11] T. Uwano and T. Itoh, "Spectral domain approach," in *Numerical Techniques for Microwave and Millimeter-Wave Passive Structures*, T. Itoh, Ed. New York: Wiley, 1989, Ch. 5, pp. 334-380.
- [12] M. Kobayashi and T. Iijima, "Frequency-dependent characteristics of current distributions on microstrip lines," *IEEE Trans. Microwave Theory Tech.*, vol. MTT-37, pp. 799-801, Apr. 1989.
- [13] E. Yamashita, K. Atsuki, and T. Ueda, "An approximate dispersion formula of microstrip lines for computer aided design of microwave integrated circuits," *IEEE Trans. Microwave Theory Tech.*, vol. MTT-27, pp. 1036-1038, Dec. 1979.
- [14] Y. X. Qian and E. Yamashita, "Phase compensation and waveform reshaping of picosecond electrical pulses using dispersive microwave transmission lines," *IEEE Trans. Microwave Theory Tech.*, vol. MTT-39, pp. 924-929, June 1991.
- [15] T. Leung and C. A. Balanis, "Attenuation distortion of transient signals in microstrips," *IEEE Trans. Microwave Theory Tech.*, vol. MTT-36, pp. 765-769, Apr. 1988.
- [16] Y. X. Qian, L. Zhu, and E. Yamashita, "Characterization of picosecond pulse propagation in a microstrip line divider," *IEEE Microwave Guided Wave Lett.*, vol. 2, pp. 191-193, May 1992.



**Yongxi Qian (S'91)** was born in Shanghai, China, on September 25, 1965. He received the B.E. degree from Tsinghua University, Beijing, China, in January 1987, and the M.E. degree from the University of Electro-communications, Tokyo, Japan, in March 1990.

He is presently with the Department of Electronic Engineering, University of Electro-communications, working toward the Ph.D. degree. His research interests include numerical analysis methods of microwave and millimeter wave transmission lines, optical generation of ultrashort electrical pulses, propagation characteristics of ultrashort electrical pulses in dispersive as well as nonlinear transmission lines, pulse crosstalk between interconnects within MMIC's and high-speed digital circuits, and picosecond characterization of microwave devices such as microstrip line dividers.

Mr. Qian is a member of the Institute of Electronics, Information, and Communication Engineers of Japan.



**Eikichi Yamashita (M'66-SM'79-F'84)** was born in Tokyo, Japan, on February 4, 1933. He received the B.S. degree from the University of Electro-communications, Tokyo, Japan, and the M.S. and Ph.D. degrees from the University of Illinois, Urbana, all in electrical engineering, in 1956, 1963, and 1966, respectively.

From 1956 to 1964, he was a member of the research staff on millimeter-wave engineering at the Electrotechnical Laboratory, Tokyo, Japan. While on leave from 1961 to 1963 and from 1964 to 1966,

he studied solid-state devices in the millimeter-wave region at the Electro-Physics Laboratory, University of Illinois. He became Associate Professor in 1967 and Professor in 1977 in the Department of Electronic Engineering, the University of Electro-communications, Tokyo, Japan. His research work since 1956 has been principally on applications of electromagnetic waves such as various microstrip transmission lines, wave propagation in gaseous plasma, pyroelectric-effect detectors in the submillimeter-wave region, tunnel-diode oscillators, wide-band laser modulators, various types of optical fibers, and ultrashort electrical pulse propagation on transmission lines. He edited the book, *Analysis Methods for Electromagnetic Wave Problems*, (Norwood, MA: Artech House).

Dr. Yamashita was Chairperson of the Technical Group on Microwaves, IEICE, Japan, for the period 1985-1986 and Vice-Chairperson, Steering Committee, Electronics Group, IEICE, for the period 1989-1990. He served as Associate Editor of the IEEE TRANSACTIONS ON MICROWAVE THEORY AND TECHNIQUES during the period 1980-1984. He was elected Chairperson of the MTT-S Tokyo Chapter for the period 1985-1986. He has been a member of the MTT-S ADCOM since January 1992. He served as Chairperson of International Steering Committee, 1990 Asia-Pacific Microwave Conference, held in Tokyo and sponsored by the IEICE.